A Region Quadtree-Based Framework for Similarity Searches of Image Databases

Charles W. Emerson[1], Sivagurunathan Chinniah[1], Nina Siu-Ngan Lam[2], and Dale A. Quattrochi[3]

[1]Department of Geography
Western Michigan University
Kalamazoo, MI 49008-5424
Tel: +1 269-387-3430
FAX: +1 269-387-3442
Email: charles.emerson@wmich.edu

[2]Louisiana State University
Department of Geography & Anthropology
Rm. 227 Howe-Russell Geoscience Complex
Baton Rouge, LA 70803
Tel: +1 225-578-6197
FAX: +1225-578-4420
Email: nlam@lsu.edu

[3]National Aeronautics and Space Administration
Earth and Planetary Science Branch XD11
National Space Science and Technology Center
320 Sparkman Drive
Huntsville, AL 35805
Tel: +1 256-961-7887
FAX: +1256-961-7788
Email: dale.quattrochi@nasa.gov

Abstract

Identifying occurrences of objects of interest in a remotely sensed digital image and finding similar objects in a database of comparable imagery usually involves a high-level semantic description based on visual interpretation of every image in the database. This work proposes a similarity search approach wherein the user identifies an object of interest, spatial and spectral characteristics of the object are calculated, and the result is compared to a database of these same calculations that have been performed on all images in the database. The spatial extent of the object of interest is approximated using a region quadtree decomposition of the image. Spatial indices such as fractal dimension, lacunarity, and Moran's I index of spatial autocorrelation, along with spectral characteristics expressed as histograms of each band's gray scale values are matched against a set of these same indices that have been previously calculated for all images in a database. The sum of squared differences between the indices calculated for the quads that form the

object of interest and the same quads in the database yields a ranked list of images that have similar characteristics. The retrieval success rate is highly dependent on the configuration of quads used to define the object of interest and the nature of the object itself. Objects such as a lake shoreline are best retrieved using the gray scale histogram, while urban features that are characterized by their texture are more accurately retrieved using indices such as fractal dimension or lacunarity.

1. Introduction

This paper describes a framework for content-based image retrieval using a region quadtree decomposition of images. In this pilot-scale utility, a Landsat scene is subsetted it into 506 512 x 512 images. A batch mode program then analyses each of these images for a number of textural indices and spectral (gray scale in the current version) characteristics. These include: box counting and triangular prism fractal dimension, Moran's *I*, lacunarity, and mean, standard deviation and a 5-bin histogram of the brightness values. These analyses are performed for six levels of quadtree decomposition of the image and the results are stored in a Microsoft Access database. In the Image Characterization and Modeling System (ICAMS)(Quattrochi, et al., 1997), the user then opens a 512 x 512 image and uses the mouse to define an object of interest using a quadtree breakdown of the image. Selected quads that correspond to the object are then analyzed for the same indices contained in the database. The software then ranks the images on how closely the corresponding quads in each of the database images match the results for the object of interest.

1.1 The Problem

Satellite and aircraft-borne remote sensors have gathered huge volumes of data over the past 30 years. In the Earth Observing System (EOS) era, terabytes of image data are being archived every day. As the geographical and temporal coverage, the spectral and spatial resolution, and the number of individual sensors increase, the sheer volume and complexity of available data sets will complicate management and use of the rapidly growing archive of earth imagery. A single scene also covers a large part of the Earth's surface, so it may take a lengthy manual search to find other occurrences of an object of interest. This paper proposes a method to facilitate analysis of either a database of separate images or specific features contained within a single image.

1.2 Data Mining

The vast amount of information on the World Wide Web would be of little use without a means to locate information on topics selected by a user. Search engines that rely on keyword matches between the query and Web page titles or other indexed data are essential for successful use of this resource. Indexing multimedia data, such as imagery, videos, and audio files have proven to be problematic (Paquet, et al., 2000). The many existing and potential uses for remotely sensed imagery make accessing images suited to a particular user's needs extremely complex and difficult. Even seemingly simple searches for images depicting a particular location involve time-consuming analyses of the many individual scenes that have been gathered over the past 30 or more years, each having different sensor platforms, levels of quality (due to cloud cover, illumination,

etc.), dates, and pre-processing. Metadata schemes such as the Earth Observing System Data and Information System (EOSDIS) Core Metadata Model (http://ecsinfo.gsfc.nasa.gov) address this to some extent by specifying location, lineage (including image processing and projection information), sensor characteristics, and other identifying characteristics to aid searches for images of specific areas at specific times. Ohm, et al., (2000) characterize these as "high-level descriptors" which are generated when raw imagery is prepared for release. Mid-level descriptors include rule-based semantic identification of objects within a scene such as lakes, mountains, and vegetated areas. Low-level descriptors are image characteristics such as shape, color, pattern, and texture. By their nature, the mid- and low-level descriptors are often user-specific, and it would not be practical to add all of this information as formal metadata, since it is impossible to anticipate all uses to which an image may be applied.

It is becoming apparent that the common practice of using general metadata structures to access specific images is ineffective, thus pointing toward a need for intelligent image query techniques (Agouris, et al., 1999). The MPEG-7 initiative aims to: a) create standards for the description of shape, color, and texture of objects depicted in audiovisual data, b) implement a description scheme, and c) provide ways of extending these descriptors and schemes via a specification language (Benitez, et al., 2000). However, unlike other forms of multimedia data, remote sensing images do have characteristics that can be captured and generalized into mid- and low-level image properties.

1.3 Content-based Image Retrieval

Content-based image retrieval is the process of selecting images from an archive based on semantic and visual contents. This necessarily involves high to low-level characteristics of the image itself (Smeulders, et al., 2000). In most of the applications reported in the pattern recognition literature (Manjunath and Ma, 1996; Datcu, et al, 2003; Yao and Chan, 2003; and Li and Narayanan, 2004), our approach, which generally use some type of supervised or unsupervised image classification technique to assist image retrieval, our approach is more automated, requiring human intervention only in the object identification stage. Image classification requires some sort of human intervention, such as the selection of training sites for supervised techniques or the linking of cluster signatures to land cover classes in the case of unsupervised classification.

2. Methodology

2.1 ICAMS

The Image Characterization and Modeling System (ICAMS) was initially developed by members of this research team (Quattrochi, et al., 1997; Lam et al., 2002) as an extension to the Arc/INFO and Intergraph MGE Geographic Information System (GIS) software packages, and it used the outdated ERDAS™ .lan file format. The recently developed ICAMS-Java version uses the latest Java Advanced Imaging (JAI) application programming interface, thus allowing the use of TIFF, GIF, JPEG, or PNG formatted images. ICAMS was developed primarily as a test-bed for evaluating the performance of

various spatial analytical methods on remotely sensed images and as such, it is intended to work with other commercially available image analysis and geographic information system (GIS) software packages. Thus, the uncompressed TIFF format is expected to be utilized most often by ICAMS users, as this is compatible with all other types of software.

ICAMS includes utilities for contrast stretching, edge detection, wavelet decomposition, and Fourier transforms. It also computes fractal dimension using the box counting, triangular prism, and isarithm methods (Jaggi, et al, 1993), and it measures lacunarity, a scale-dependent measure of the gaps in an imaged pattern (Dong, 2000). The application also includes utilities for measuring Moran's *I* and Geary's *C* indices of spatial autocorrelation (Cliff and Ord, 1973). In addition to these global (whole image or user-defined region of interest) measures, ICAMS includes local measures of triangular prism fractal dimension (Clarke, 1986), Moran's *I*, Geary's *C*, and Getis' *G* and *G** indices of spatial autocorrelation (Getis and Ord, 1992). These local measures compute the values of these indices in a moving window, thus producing an output image that shows the differences in spatial complexity across a scene.

The ICAMS feature that is the subject of this paper is the similarity search capability in which the user defines an object of interest, the application computes the spatial and spectral characteristics of this object and searches a metadata table for similar characteristics which indicate the presence of matching objects. A separate application computes the fractal dimension by box counting and triangular prism methods, Moran's I, lacunarity, and mean and standard deviation of the gray-scale values for an image database using a multi-resolution quadtree decomposition. ICAMS computes these indices for the object of interest and retrieves matching images from the index database.

2.2 Feature-Based Similarity Search

Figure 1 shows the procedure used in this example. A Landsat 7 ETM+ panchromatic image obtained on October 24, 2000 was subsetted into 512 x 512 pixel images to form an example image database. The Landsat scene (Path 19, Row 36) includes the northern half of the Atlanta, Georgia metropolitan area, plus the southern end of the Appalachian Mountains in North Georgia, Alabama, North Carolina and Tennessee (Figure 2). The scene includes a range of land covers including extensive areas of forested mountains and the northern suburbs of Atlanta, some large lakes, and smaller areas of pasture lands.

Textural and gray scale characteristics of each of these 512 x 512 pixel images was analyzed in a recursive region quadtree structure (Samet, 1984), in which the results from progressively smaller square regions are stored in a relational database of image indices. An example object of interest contained in a 512x512 image is defined by a quadtree decomposition of the image. Figure 3 shows how quads that correspond to the object are indexed within the region quadtree structure. The user clicks on the image to break it down into progressively smaller segments. Figure 4 shows an example object of interest that has been defined in this fashion, with the quads corresponding to the object selected by a right-click.

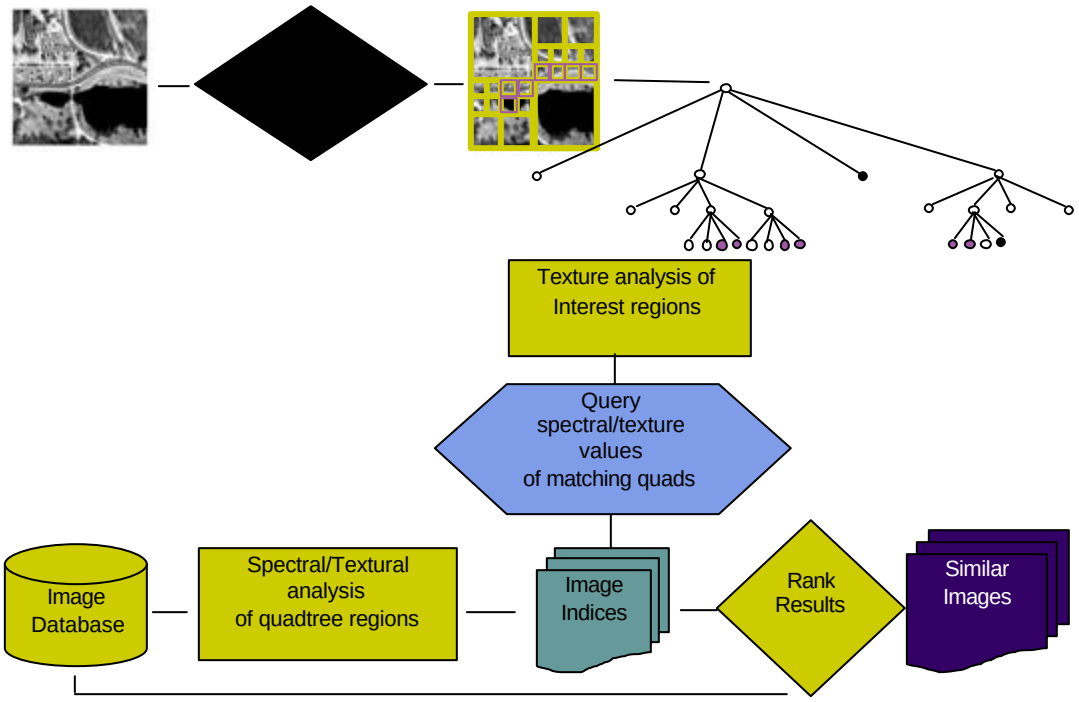

Figure 1. Content based image retrieval process.

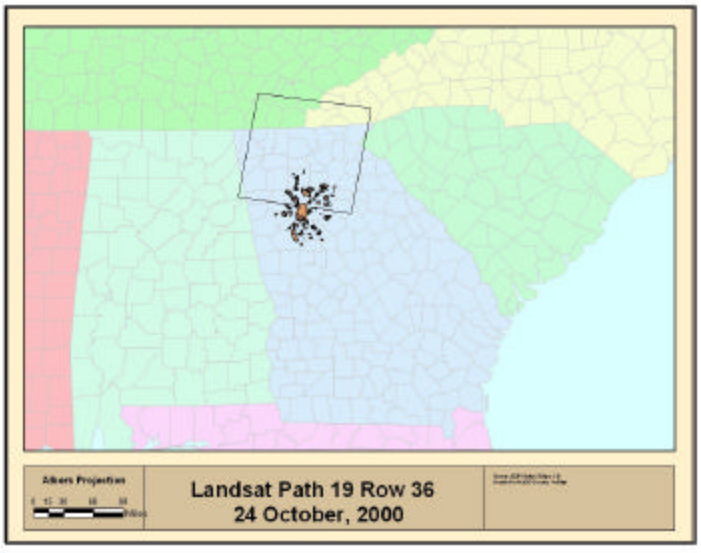

Figure 2. Footprint of Landsat image showing Atlanta metropolitan area.

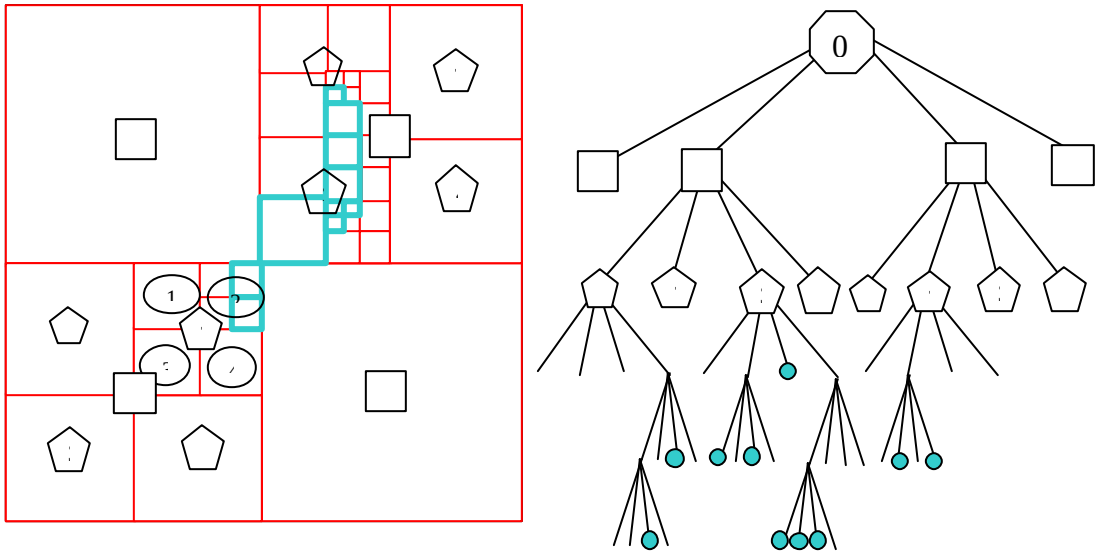

Figure 3. Region quadtree map and tree structure for user defined object.

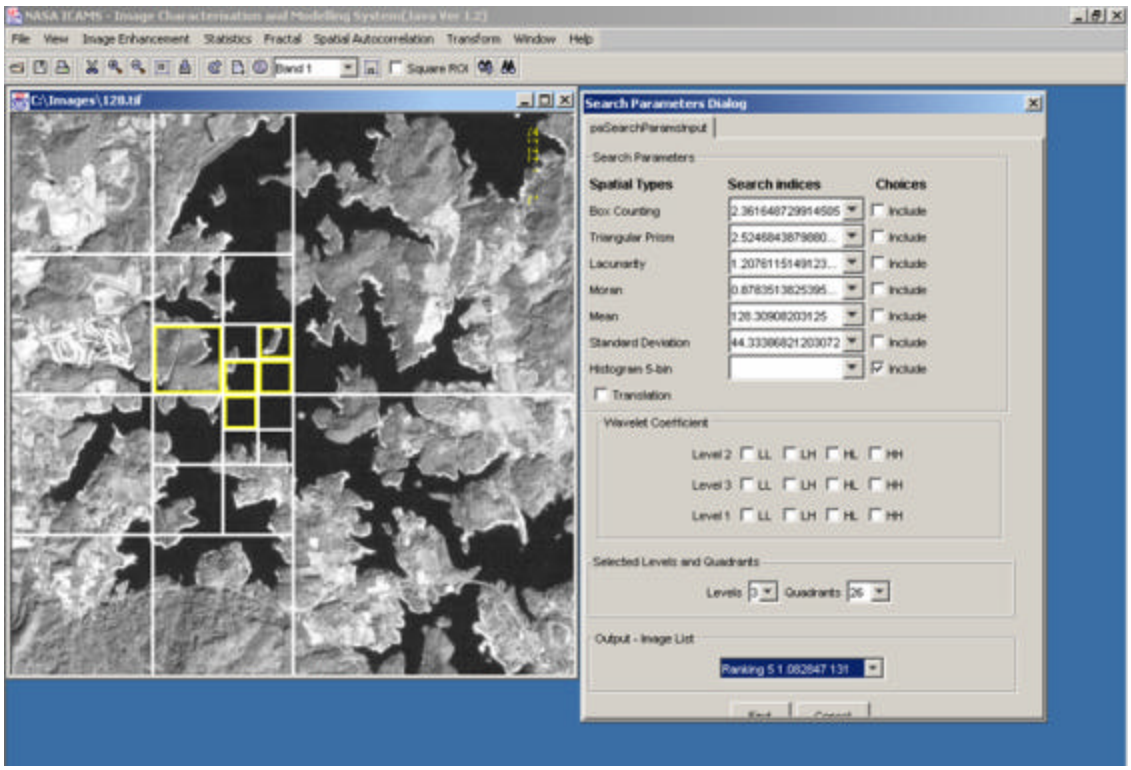

Figure 4. Region quadtree feature selection in ICAMS. (quads for user-defined object are highlighted in yellow).

2.3 Indices

Each image was analyzed using a number of textural indices including: fractal dimension by the triangular prism method, fractal dimension by box counting, and Moran's I index of spatial autocorrelation. Descriptive statistics of the gray scale digital numbers included: mean, standard deviation, and a 5-bin normalized histogram.

2.3.1 Fractal Dimension

Fractal analysis (Mandelbrot, 1983) provides tools for measuring the geometric complexity of imaged objects. In Euclidean space, a point has an integer topological dimension of zero, a line is one-dimensional, an area has two dimensions and a volume has three. The *fractal dimension* (*D*), however, is a non-integer value that, in Mandelbrot's (1983) definition for fractals, exceeds the topological dimension as the form of a point pattern, a line, or an area feature grows more geometrically complex. The fractal dimension of a point pattern can be any value between zero and one, a curve, between one and two, and a surface, between two and three. Increasing the geometrical complexity of a perfectly flat two-dimensional surface ($D = 2.0$) so that the surface begins to fill a volume, results in *D* values approaching 3.0.

ICAMS-Java has three methods of measuring fractal dimension of a gray-scale image surface: the triangular prism method (Clarke, 1986), the isarithm method (Lam and De Cola, 1993) and the box counting method (Liebovitch and Toth, 1989; Sarkar and Chaudhuri, 1992). The triangular prism method constructs triangles by averaging the *z*-values (which in this case are the digital numbers) for sets of four adjacent pixels. The *z*-values for each pixel are used to establish heights at each corner, and triangles are formed by connecting these corner values to the mean value of the four pixels at the center of the array (Figure 5).

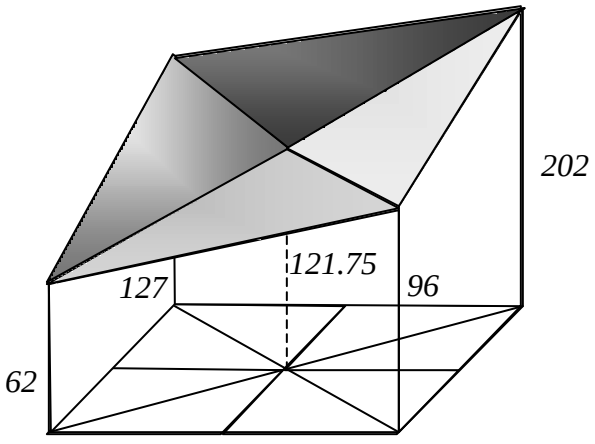

Figure 5. Triangular prism

Figure 6 shows an example 7 x 7 array of pixel values. In step 1, the areas of all triangles formed by 2 x 2 arrays of pixels are computed. The areas of the triangular "facets" of the prisms are then summed to represent the total step 1 surface area. The algorithm then steps to 3 x 3 arrays of pixels, with the center height corresponding to the average of the

four corners. The algorithm continues to increase the pixel size and compute the triangular prism areas until the entire surface is calculated as a single composite array. The logarithm of the total of all the prism facet areas at each step is plotted against the logarithm of the pixel dimension (integer multiples of 15 m for Landsat ETM+ panchromatic) at each step. The fractal dimension is calculated by performing a least squares regression on the surface areas and pixel sizes. The regression slope B is used to determine the fractal dimension D, where $D = 2 - B$.

In the box counting fractal dimension measurement method, the image is considered to be a 3-dimensional space, with x and y being the column and row of the pixels, and the z value corresponding to the 8-bit gray scale value of the pixel. Figure 7 shows an image grid with one row of 3 pixels depicted in this fashion. If we stack a series of 3-Dimensional boxes of pixel dimension r (r = 3 in Figure 7), so that the maximum z values are covered by the boxes at each x,y location, we can then determine the number of boxes needed to span the gray-scale values from the minimum to the maximum values. The total count of boxes needed to span all of the gray scale values throughout the image (N_r) is summed in Equation 1 as:

$$N_r = \sum_{i,j} n_r(i, j) \tag{1}$$

where n_r is the number of boxes needed to span the gray scale values at row, column location (i,j). We compute d, the capacity, using a range of values of r and Equation 2:

$$d = \frac{\log(N_r)}{\log(1/r)} \tag{2}$$

The slope of the least squares linear line b that best fits the computed values of d for a range of box sizes is the fractal dimension D, where $D = 2 - b$.

2.3.2 Lacunarity

Lacunarity is a scale-dependent measure that is related to fractal dimension, but instead focuses on the distribution of gaps in a pattern. Low lacunarity geometric objects are homogeneous, with similar gaps occurring at regular intervals if they occur at all. High lacunarity objects have an irregular arrangement of gaps. Since homogeneous patterns can appear heterogeneous over large spatial extents, lacunarity is scale-dependent. The method for measuring lacunarity in ICAMS-Java is derived from the gliding box algorithm proposed by Allain and Cloitre, (1991), and developed by Plotnick, et al., (1996). Dong (2000) extended the gliding box technique to gray-scale images.

The gliding box method is similar to the box counting method described above, except in the case of lacunarity, $Q(M,r)$, the probability function for the number of boxes of size r (called the mass, M) is calculated and used in Equation 3 to estimate the lacunarity ? :

$$\Lambda(r) = \frac{\sum_M M^2 Q(M, r)}{\left[\sum_M M Q(M, r)\right]^2} \tag{3}$$

58	42	55	119	201	245	240
41	51	52	62	115	189	224
40	49	59	62	65	87	135
46	36	46	68	66	50	61
100	55	29	44	62	56	46
199	153	88	44	37	48	52
221	216	179	110	50	30	41

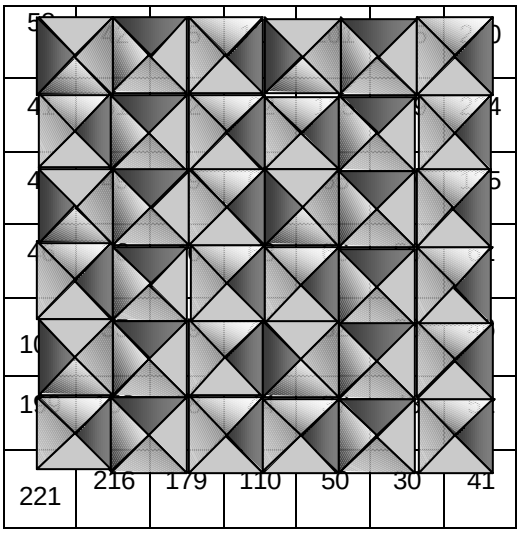

58	42	55	119	201	245	240
41	51	52	62	115	189	224
40	49	59	62	65	87	135
46	36	46	68	66	50	61
100	55	29	44	62	56	46
199	153	88	44	37	48	52
221	216	179	110	50	30	41

58	42	55	119	201	245	240
41	51	52	62	115	189	224
40	49	59	62	65	87	135
46	36	46	68	66	50	61
100	55	29	44	62	56	46
199	153	88	44	37	48	52
221	216	179	110	50	30	41

Fi[illegible]ular Prism[illegible]m

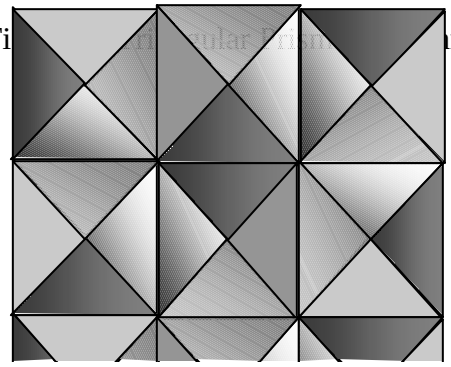

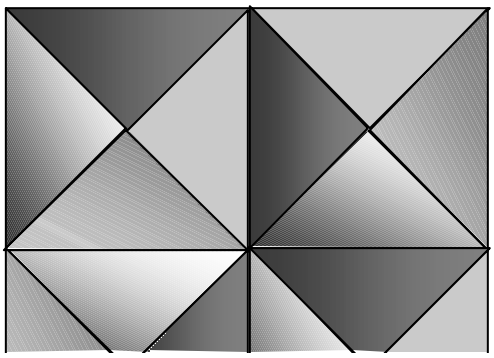

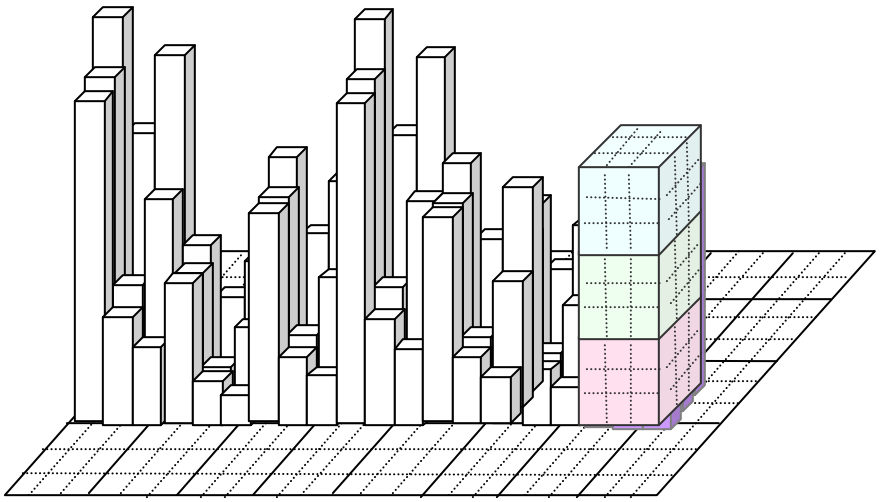

Figure 7. Box Counting Method of Measuring Fractal Dimension

2.3.3 Moran's I

In addition to variograms and fractal dimensions, spatial autocorrelation of raster images can be characterized by join count statistics such as Moran's *I* and Geary's *C* (Cliff and Ord, 1973), which reflect the differing spatial structures of the smooth and rough surfaces. Moran's *I* varies from +1.0 for perfect positive correlation (a clumped pattern) to –1.0 for perfect negative correlation (a checkerboard pattern).

ICAMS also contains modules for analyzing the spatial autocorrelation of images. Moran's *I*, Geary's *C*, and Getis' G, three indices of spatial autocorrelation, reflect the differing spatial structures of the smooth and rough surfaces. Moran's *I* is calculated using Equation 4:

$$I(d) = \frac{n \sum_{i}^{n} \sum_{j}^{n} w_{ij} z_i z_j}{W \sum_{i}^{n} z_i^2} \qquad (4)$$

where w_{ij} is the weight at distance d, so that, $w_{ij} = 1$ if point j is within distance d from point i, otherwise $w_{ij} = 0$; z's are deviations (i.e., $z_i = x_i - x_{mean}$ for variable x), and W is the sum of all the weights where $i \neq j$. Moran's *I* varies from +1.0 for perfect positive correlation (a clumped pattern) to –1.0 for perfect negative correlation (a checkerboard pattern). In this example we did not find Moran's *I* to be very helpful in image retrieval, possibly due to the narrow range of values (-1 to +1) for the standardized version of the statistic used to analyze the quads.

2.3.4 Grayscale Histogram

A 5-bin histogram of the grayscale values contained in each quad and stored in five fields in the index database. In order to facilitate comparisons between different levels of the quadtree structure with the different numbers of pixels in each level's quads, the histogram was normalized by converting each frequency bin to a percentage of total pixels in the quad. The 5-bin histogram then was considered as a group of values in the least squares comparison and ranking of results.

3. Results

3.1 Static Feature Matching

In static feature matching, the simplest form of image retrieval, the image index database is queried for the same quads in the same orientation and location as the user-defined definition of the object of interest. Corresponding quads in each of the 506 images are compared to the object definition, and the results are ranked using a least squares comparison of the identified spectral or textural indices.

In this example, two different objects were identified: (1) a collection of quads that define a lake shore or river bank with a land/water contrast, and (2) an extensive residential area.

Figure 8 shows the original query image of an area with a characteristic land/water contrast and the object definition for a 5-bin gray scale histogram analysis. The images with the top five closest matches to the query image are contained in figures 8b. through 8f. Other than the mismatch of figure 8e. (caused by the strong mountain shadow having similar gray scale values to the water bodies), the histogram works well at retrieving objects having strong spectral contrast. Table 1 shows that for this type of object, the 5-bin histogram outperformed the other indexes at image retrieval.

The heterogeneity of urban land covers makes summary statistics of gray scale values of relatively little use, since a diverse range of land cover types may have similar gray scale distributions. Table 2 shows that lacunarity yielded the highest number of land/water contrast matches in the top five ranked images, followed by fractal dimension by box counting. Figure 9 shows that four of the top five images in the lacunarity analysis matched residential areas. The mismatch occurred in a mountainous area with small water bodies, cleared areas, shadows and other features that form a complex land cover that has a complex texture similar to an urban area.

3.2 Translation, Rotation, and Scaling

Content-based image retrieval that poses other challenges, such as translation of the *x*,*y* location of matching objects in other images, rotation of the object, scaling up or down in size, isolation of the object from other patterns and textures, and 3-D orientation of the object with respect to the observer (termed "object pose" in the pattern recognition literature). However, the region quadtree structure allows at least partial ability to minimize some of these problems. With regard to translation, it is possible to search

other parts of the database images by moving the selected quads around in increments of the biggest quad in the object definition (see Figure 10). 90 degree rotations and reflections can easily be calculated within the quadtree object definition by simply changing the numbering of the nodes, although other types of rotations pose a difficult challenge (Figure 11). Scaling at integer multiples defined by the quadtree structure are simply performed by jumping up or down within the quadtree (Figure 12). The viewing angle problem is generally not severe for aircraft and satellite imagery, since the perspective is always pretty much the same (though minor adjustments have to be considered for objects significantly off-nadir).

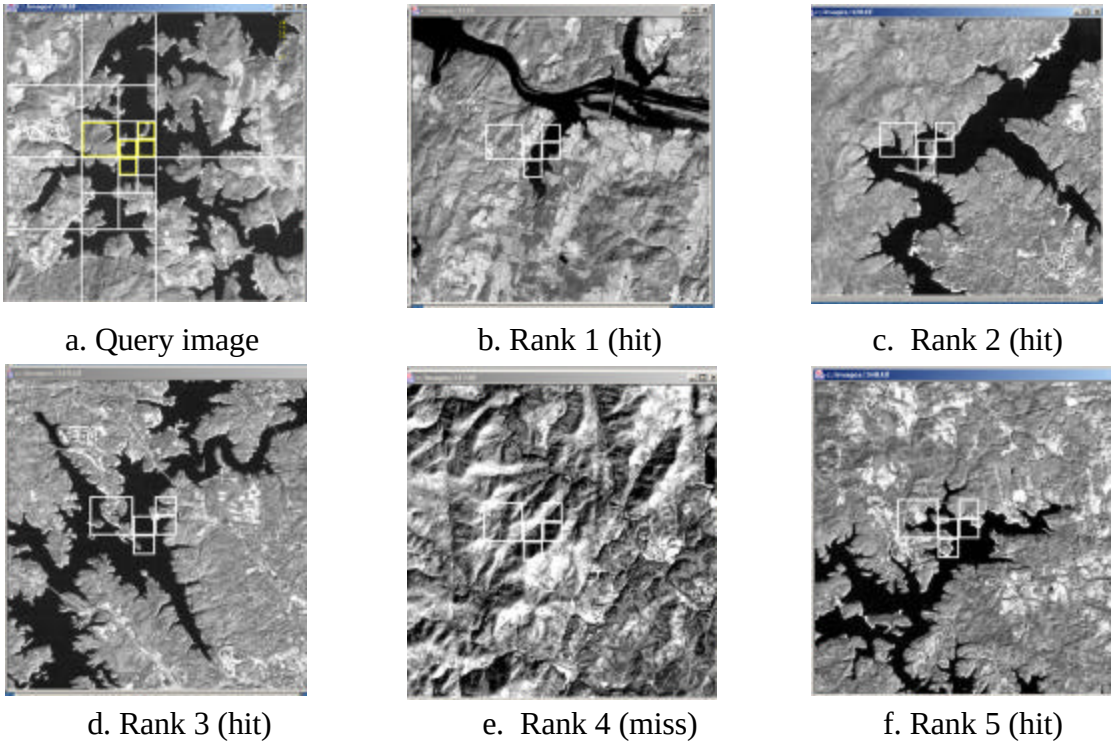

a. Query image b. Rank 1 (hit) c. Rank 2 (hit)

d. Rank 3 (hit) e. Rank 4 (miss) f. Rank 5 (hit)

Figure 8. Lake shore search using 5-bin histogram.

Table 1. Comparison of image comparison indices for the top five ranked land/water contrasts.

Index	Matches
Box Counting	1/5
Triangular Prism	0/5
Lacunarity	1/5
Moran's I	0/5

Mean	2/5
Std. Deviation	1/5
5-bin Histogram	4/5

Table 2. Comparison of image comparison indices for the top five ranked residential areas.

Index	Matches
Box Counting	3/5
Triangular Prism	2/5
Lacunarity	4/5
Moran's I	0/5
Mean	0/5
Std. Deviation	0/5
5-bin Histogram	2/5

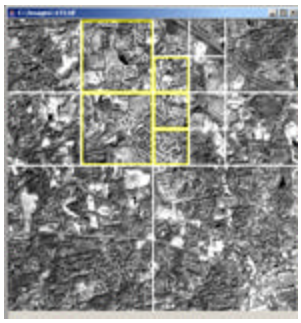

a. Query image

b. Rank 1 (miss)

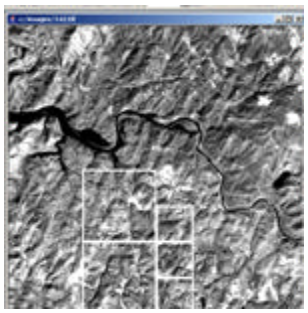

c. Rank 2 (miss)

d. Rank 3 (Commercial - miss)

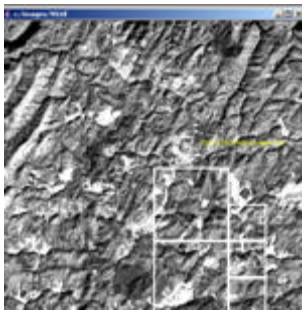

e. Rank 4 (miss)

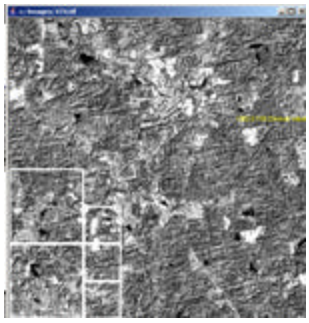

f. Rank 5 (hit)

Figure 9. Residential area matches using 5-bin histogram.

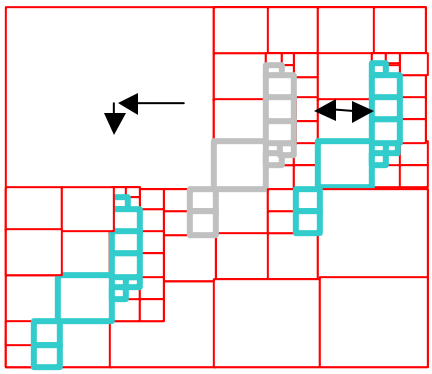

Figure 10. Translation of user defined object.

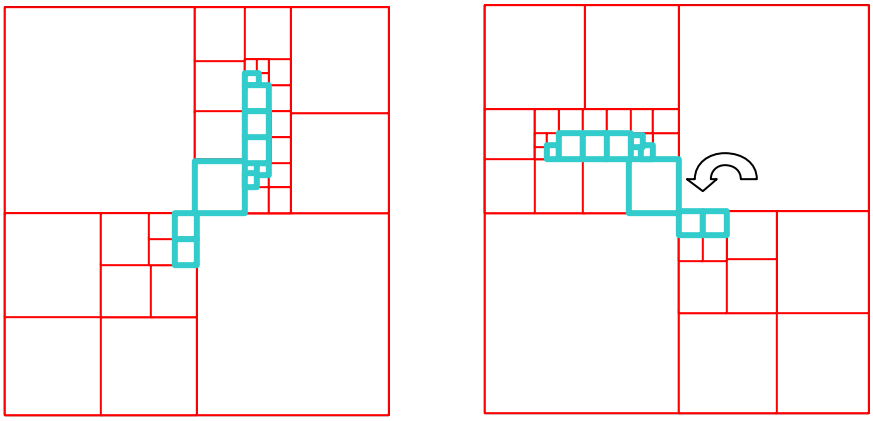

Figure 11. Rotation of user defined object.

Rotation and scaling have not yet been incorporated into the ICAMS content-based image retrieval utility. However, in the current implementation of ICAMS, translation is taken into account by moving the user defined set of quads around the entire range of possible locations of the largest quad in the object definition (Figure 10). This increases the search time, especially if the object definition does not include any large quads. Allowing the object definition to translate across the image increased the success of the image retrieval process (Table 3). Figure 13 shows that the 5-bin histogram returned matches in all five of the top ranked land/water contrast images. A quantitative determination of the success or failure of a content-based image retrieval process necessarily involves a degree of subjectivity. In this case, the database of 506 subsetted images was visually inspected for land/water contrast areas, and it was found that 62 of

the 506 images contained a matching feature. A Mann-Whitney test was performed on the ranks of all remaining 505 images in the database. Matches from the visual inspection of the database were coded as a binary grouping variable (0 = no land/water, 1 = land/water interface). Tables 4 and 5 show that the results of this analysis yield Mann-Whitney U, Wilcoxon W and Z score statistics that show the overall rankings from the 5-bin histogram were not likely to resemble those derived from a chance arrangement.

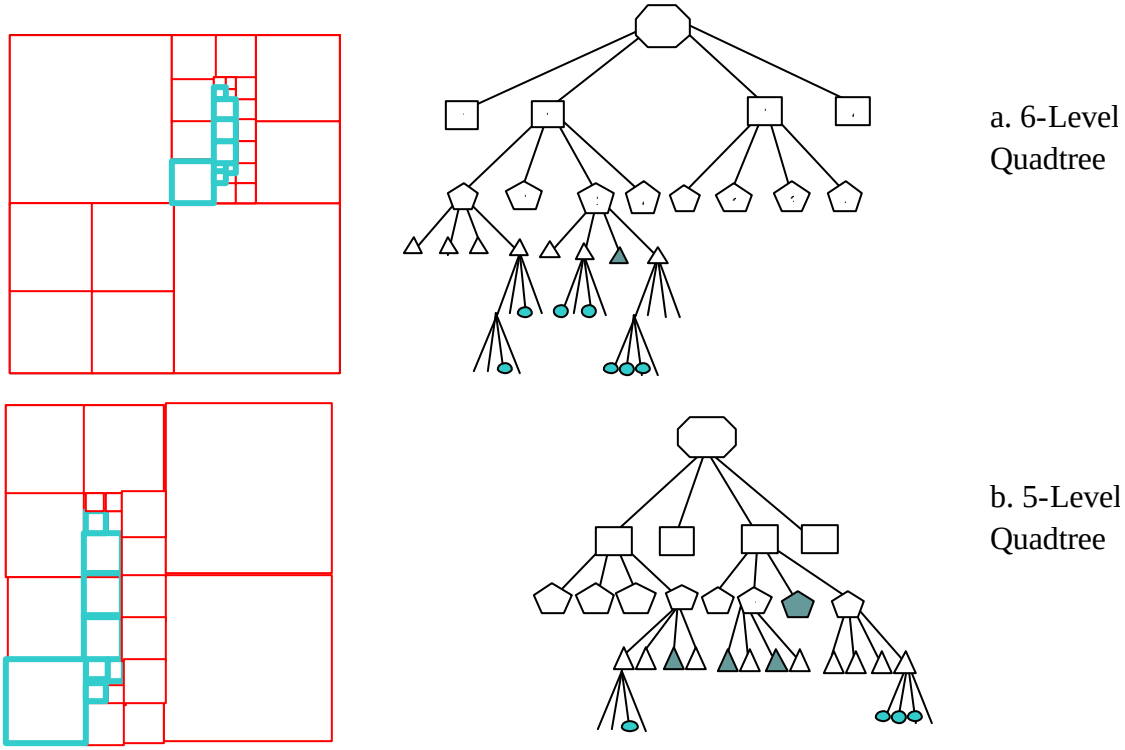

a. 6-Level Quadtree

b. 5-Level Quadtree

Figure 12. Scaling up user defined object according to quadtree hierarchy.

Table 3. Comparison of image comparison indices for the top five ranked land/water contrasts.

Index	Lake w/Translation	Res. Area w/Trans.
Box Counting	1/5	4/5
Triangular Prism	1/5	2/5
Lacunarity	1/5	4/5
Moran's I	1/5	1/5
Mean	2/5	0/5
Std. Deviation	2/5	0/5
5-bin Histogram	5/5	1/5

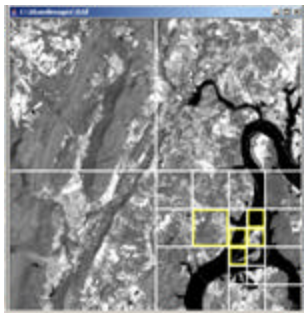

a. Query image

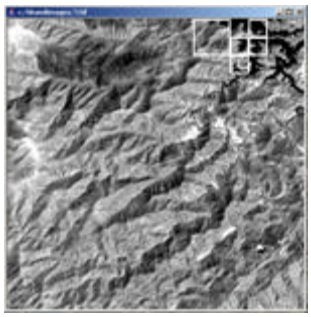

b. Rank 1 (hit)

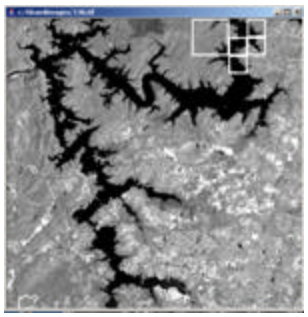

c. Rank 2 (hit)

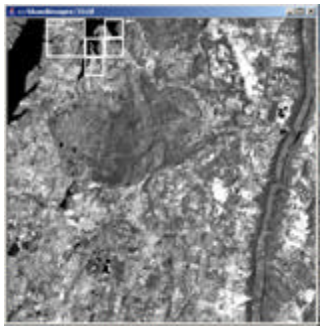

d. Rank 3 (hit)

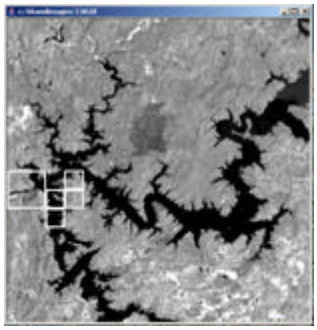

e. Rank 4 (hit)

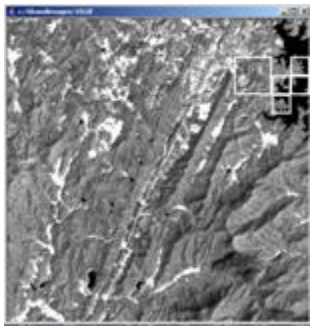

f. Rank 5 (hit)

Figure 13. Lake shore search using 5-bin histogram with translation.

Table 4. Ranks of 5-bin histogram analysis of land/water contrast

Group	N	Mean Rank	Sum of Ranks
No Land/Water	444	273.39	121385.00
Land/Water	61	104.59	6380.00
Total	505		

Table 5.Mann-Whitney test statistics of land/water analysis

Statistic	Value
Mann-Whitney U	4489.00
Wilcoxon W	6380.00
Z	-8.471
Asymp. Sig. (2-tailed)	0.000

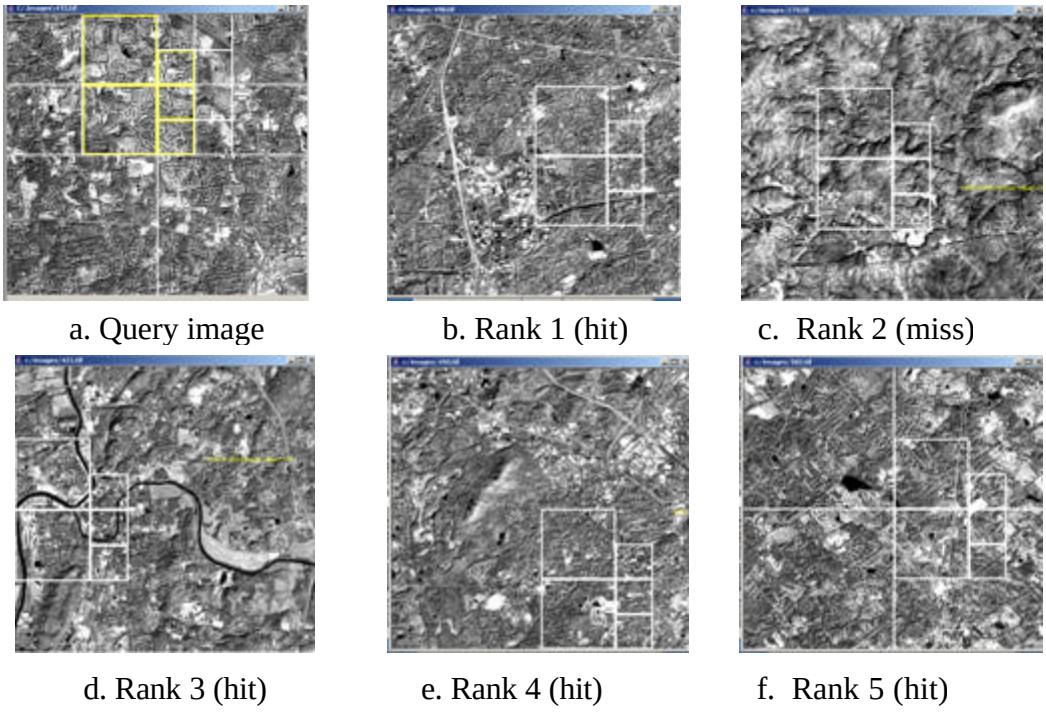

a. Query image b. Rank 1 (hit) c. Rank 2 (miss)

d. Rank 3 (hit) e. Rank 4 (hit) f. Rank 5 (hit)

Figure 14. Residential area with translation (box counting fractal dimension).

Images of urban areas are often more complex than natural landscape images, with a number of land covers closely interspersed. Residential areas are particularly difficult to pick out from other land covers, since lawns and street trees resemble grasslands and forests, and the built up areas are often difficult to distinguish from more intensive commercial land uses. Although small residential areas are dispersed throughout the Landsat scene, extensive areas corresponding to quads of 128 x 128 pixels (approximately 37 hectares) are concentrated in the Atlanta metropolitan area. From visual inspection, 69 of the 506 images had extensive residential areas. Figure 14 shows that the box counting fractal dimension successfully retrieved residential areas in four of the top five images. The retrieval efficacies of lacunarity and box counting fractal dimension were compared using the Mann-Whitney test. Tables 6 and 7 show that both methods were significantly different from random rankings, with the box counting fractal dimension having a slightly lower mean rank of residential area matches.

Table 6. Ranks of box counting fractal dimension and lacunarity analysis of residential areas.

Method	Grouping	N	Mean Rank	Sum of Ranks
Lacunarity	No Residential	438	278.10	121807.00
	Residential	67	88.93	5958.00
	Total	505		
Box Counting	No Residential	438	278.26	121878.99
	Residential	67	87.85	5886.00
	Total	505		

Table 7. Mann-Whitney test statistics of residential area analysis.

Statistic	Lacunarity	Box Counting
Mann-Whitney U	3680.00	3608.00
Wilcoxon W	5958.00	5886.00
Z	-9.882	-9.947
Asymp. Sig. (2-tailed)	0.000	0.000

4. Conclusions

Although the basic framework for performing content-based image retrieval is presently encoded into ICAMS-Java, there still remains much to accomplish before the tool can be considered successful. Major challenges are: developing a better user interface for outlining the feature of interest, finding improved ways to formulate the database query; properly weighting the different indices; and establishing a more efficient ranking of the images for retrieval. The current version uses the sum of squared differences between the indices in the user defined object and the corresponding quads in the database for each image. Currently, only single-band images can be analyzed at this point, and this limits the accuracy of the retrieval. Adding multispectral capability should significantly improve performance, since many of the key identifying characteristics of objects are related to color (Yao and Chen, 2003), as represented by the information contained in multispectral bands.

We have found that the quadtree structure provides a good basis for a user to isolate the object of interest from the background if the user selects regions that characterize the object itself and it is often useful to select surrounding regions that are not part of the defined object. The quadtree structure also provides an efficient means of indexing and searching a database of low level image characteristics. Some of the indices that have

been examined in this work, most particularly fractal dimension and lacunarity, are greatly affected by the statistical support (size) of the selected quads, and this both encourages the use of larger quads and simultaneously leads to a more approximate definition of the complex shape of a defined object.

Basically this region quadtree approach provides a framework for evaluating the performance of potentially any combination of textural or spectral measures for content-based image retrieval. Pre-processing a large image scene or a collection of scenes and storing the spatial and spectral indices in a database can potentially extend the definition of metadata beyond the usual descriptions of acquisition date, sensor identification, and lineage to a richer content-based description that can facilitate access to imagery that depicts specific objects and conditions on the Earth's surface that may be of interest to researchers engaged in earth science, resource development, planning, and security investigations.

5. Acknowledgements

This research is supported by a research grant from NASA Intelligent Systems research grant (NAS-2-37143).

6. References

Agouris, P., Carswell, J. and Stefanidis, A. 1999. An environment for content-based image retrieval from large spatial databases. *ISPRS Journal of Photogrammetry and Remote Sensing*, **54**:263-272.

Allain, C. and Cloitre, M., 1991, Characterizing the lacunarity of random and deterministic fractal sets. *Physical Review A*, **44**, 3552-3558.

Benitez, A.B., P. Seungyup, S. Chang, A. Puri, Q. Huang, J.R. Smith, C. Li, L.D. Bergman, C.N. Judice, 2000. Object-based multimedia content description schemes and applications for MPEG-7, *Signal Processing: Image Communication*, 16:235-269.

Clarke, K., 1986, Computation of the fractal dimension of topographic surfaces using the triangular prism surface area method. *Computers and Geosciences*, **12**, 713-722.

Cliff, A. and Ord, J., 1973. *Spatial Autocorrelation* (London: Pion Limited).

Datcu, M., Daschiel, H., Pelizzari, A., Quartulli, M., Galoppo, A., Colapicchioni, A., Pastori, M., Seidel, K., Marchetti, P., and D'Elia, S., 2003, Information mining in remote sensing image archives: system concepts, *IEEE Transactions on Geoscience and Remote Sensing*, **41**(12), 2923-2936.

Dong, P., 2000, Test of a new lacunarity estimation method for image texture analysis. *International Journal of Remote Sensing*, **21**(17), 3369-3373.

Getis, A. and Ord, J., 1992. The analysis of spatial association by the use of distance statistics. *Geographical Analysis*, **24**:189-206.

Jaggi, S., Quattrochi, D., and Lam, N., 1993, Implementation and operation of three fractal measurement algorithms for analysis of remote-sensing data. *Computers and Geosciences*, **19**, 745-767.

Lam, N. and De Cola, L., eds., 1993. *Fractals in Geography* (Englewood Cliffs, NJ: Prentice Hall).

Lam, N., Qiu, H., Quattrochi, D., Emerson, C., 2002, An evaluation of fractal methods for characterizing image complexity. *Cartography and Geographic Information Science*, **29**, 25-35.

Li, J. and Narayanan, R., 2004, Integrated spectral and spatial information mining in remote sensing imagery, *IEEE Transactions on Geoscience and Remote Sensing*, **42**(3), 673-685.

Liebovitch, L. and Toth, T., 1989. A fast algorithm to determine fractal dimensions by box counting, *Physics Letters A*, **141**(8,9):386-390.

Mandelbrot, B., 1983. *The Fractal Geometry of Nature* (New York: W.H. Freeman and Co).

Manjunath, B. and Ma, Y., 1996, Texture features for browsing and retrieval of image data, *IEEE Transactions on Pattern Analysis and Machine* Intelligence, **18**(8): 837-842.

Ohm, J.R., Bunjamin, F., Liebsch, W., Makai, B., Muller, K., Smolic, A., Zier,D., 2000. A set of visual feature descriptors and their combination in a low-level description scheme. *Signal Processing: Image Communication*., **16**:157-179.

Paquet, E., Rioux, M., Murching, A., Naveen, T., and Tabatabai, A., 2000. Description of shape information for 2-D and 3-D objects. *Signal Processing: Image Communication*, **16**:103-122.

Plotnick, R., Gardner, R., Hargrove, W., Prestegaard, K., Perlmutter, M., 1996, Lacunarity analysis: a general technique for the analysis of spatial patterns. *Physical Review E*, **53**(5), 5461-5468.

Quattrochi, D., Lam, N., Qiu, H., and Zhao, W., 1997. Image characterization and modeling systems (ICAMS): A geographic information system for the characterization and modeling of multiscale remote sensing data. In *Scaling in Remote Sensing and GIS*. D. Quattrochi and M. Goodchild, eds., pp. 295-307. Boca Raton, Florida: CRC/Lewis Publishers.

Samet, H., 1984, The quadtree and related hierarchical data structures. *Computing Surveys*, **16**(2), 187-260.

Sarkar, N. and Chaudhuri, B., 1992. An efficient approach to estimate fractal dimension of textural images, *Pattern Recognition*, **25**(9):1035-1041.

Smeulders, A., Worring, M., Santini, S., Gupta, A., and Jain, R., 2000, Content-based image retrieval at the end of the early years, *IEEE Transactions on Pattern Analysis and Machine Intelligence*, **22**(12), 1349-1380.

Yao, C. and Chen, S., 2003, Retrieval of translated, rotated and scaled color textures, *Pattern Recognition*, **36**, 913-929.